Supplementary Figures

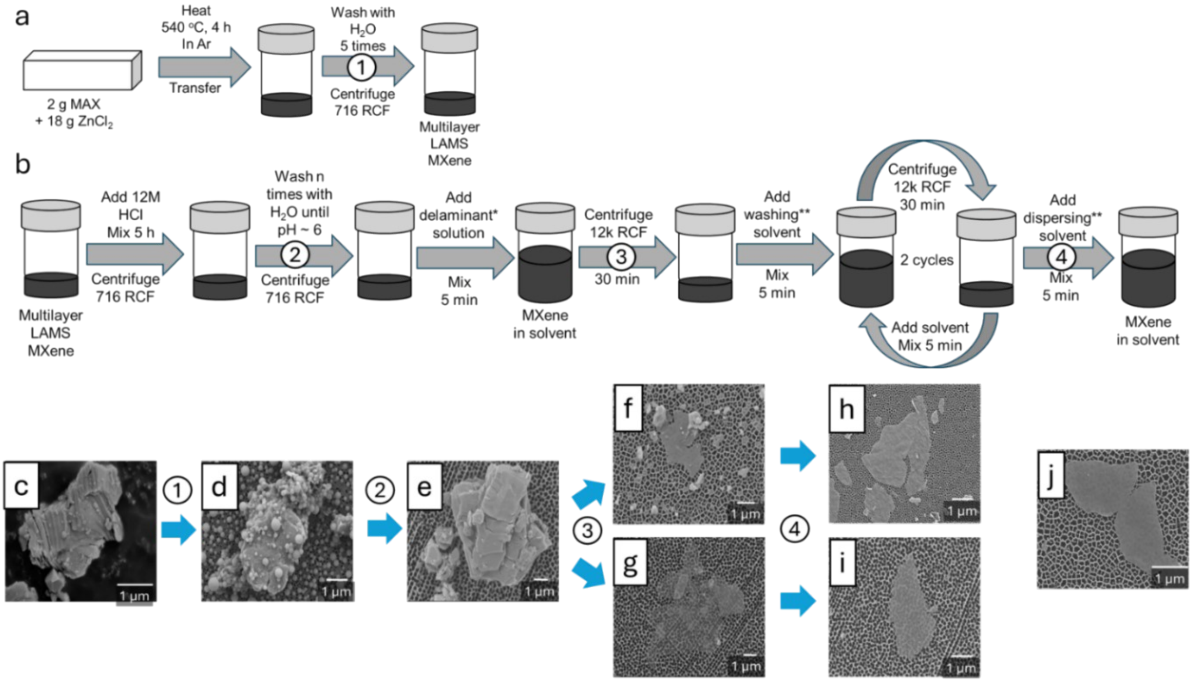

Fig. S1. (a) Illustration of the LAMS etching process and (b) the subsequent solution-based delamination of MXenes. Scanning electron microscopy images of (c) Ti_3AlC_2 MAX phase precursor; (d) multilayer MXene after sintering; (e) multilayer Cl-MXene after washing with 12 M HCl and water; (f) single-layer Cl-MXene along with multilayer impurities after delamination; (g) single-layer O,Cl-MXene (with few multilayer impurities) after delamination; (h) single-layer Cl-MXene (with few multilayer impurities) after further washing; (i) single-layer O,Cl-MXene after further washing; and (j) single-layer MILD-MXene.

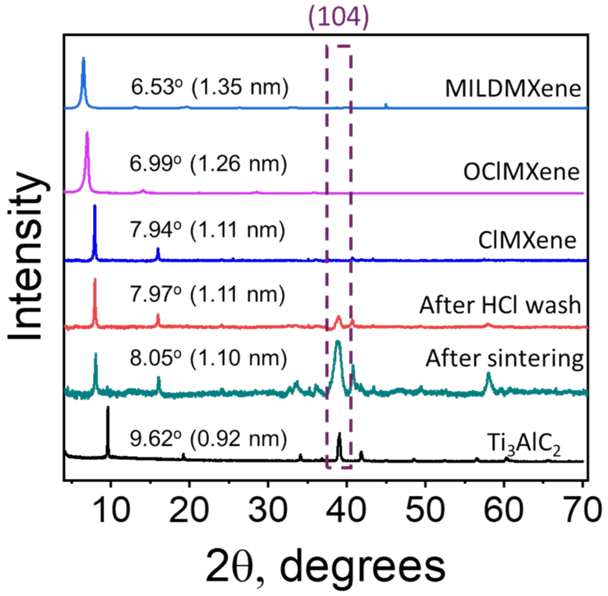

Fig. S2. X-Ray diffractograms for the LAMS synthesis of Cl-MXene and O,Cl-MXene at each synthesis step. Delaminated MILD-MXene was added for comparison.

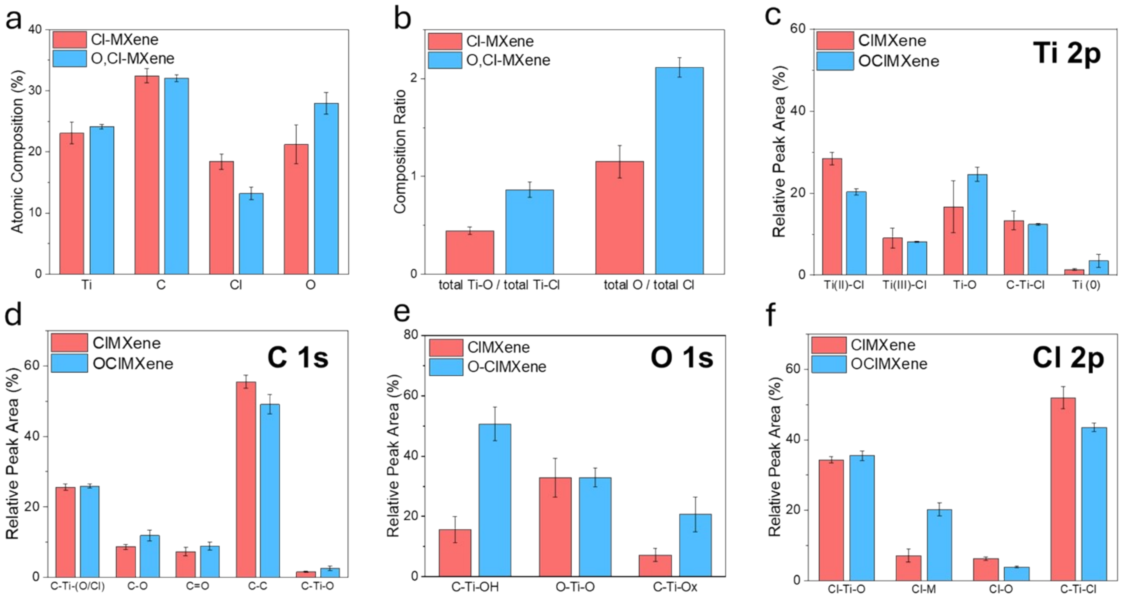

Fig. S3. (a) Percentage elemental distribution of Ti, C, Cl, and O for the MXene samples. (b) Calculated ratios of the Ti-O/Ti-Cl and total O/Cl for both Cl-MXene and O,Cl-MXene based on total relative atomic compositions. Relative peak areas of the chemical bonds derived from high-resolution XPS core-level spectra of (c) Ti 2p, (d) C 1s, (e) O 1s, (f) Cl 2p.

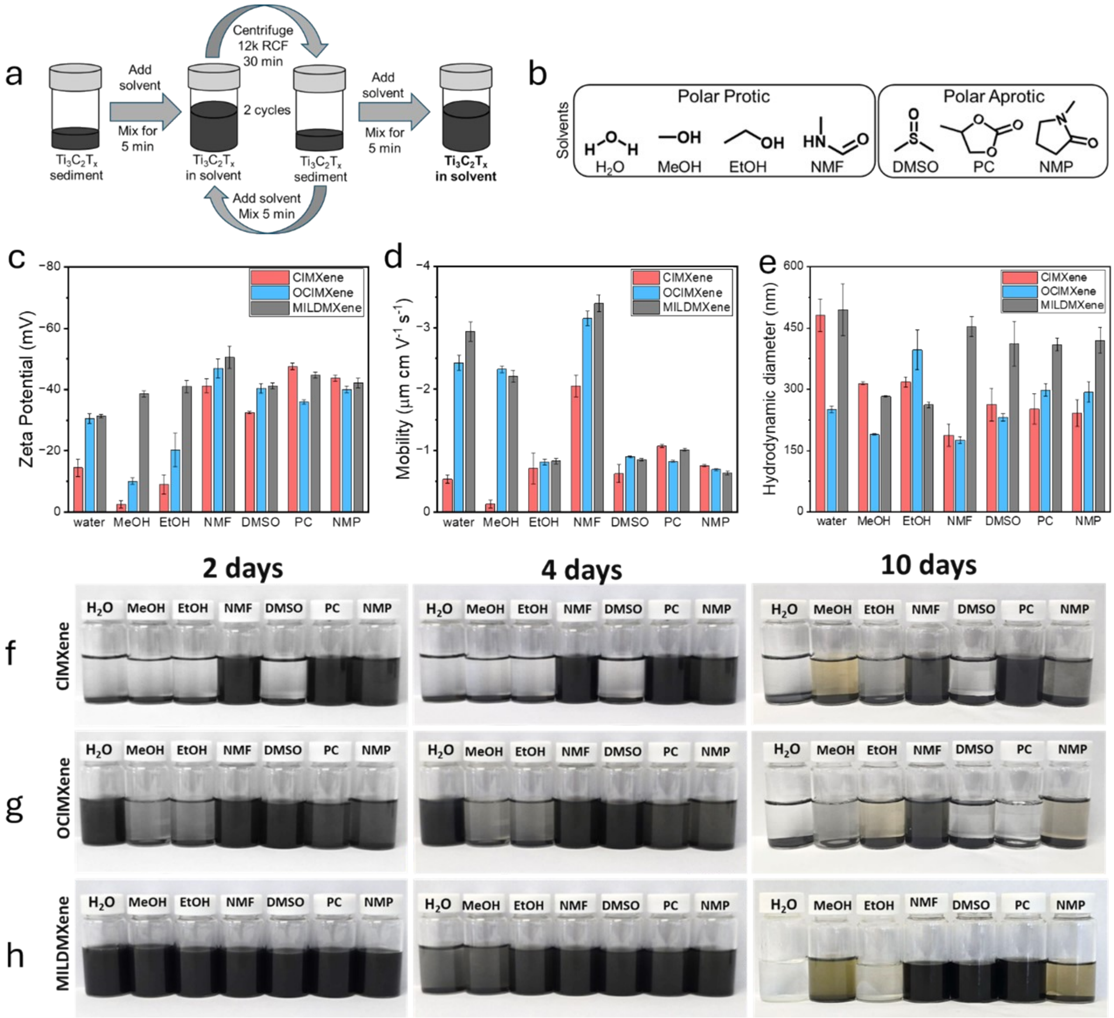

Fig. S4. (a) Solvent exchange method used for the MXene dispersions. (b) Solvents used for dispersion experiments. Zeta potential (c), mobility (d), and hydrodynamic diameter (e) values of the MXene dispersions. ClMXene (f), OClMXene (g), and MILDMXene (h) dispersions (5 mg mL^{-1}) after standing undisturbed after 2, 4, and 10 days.

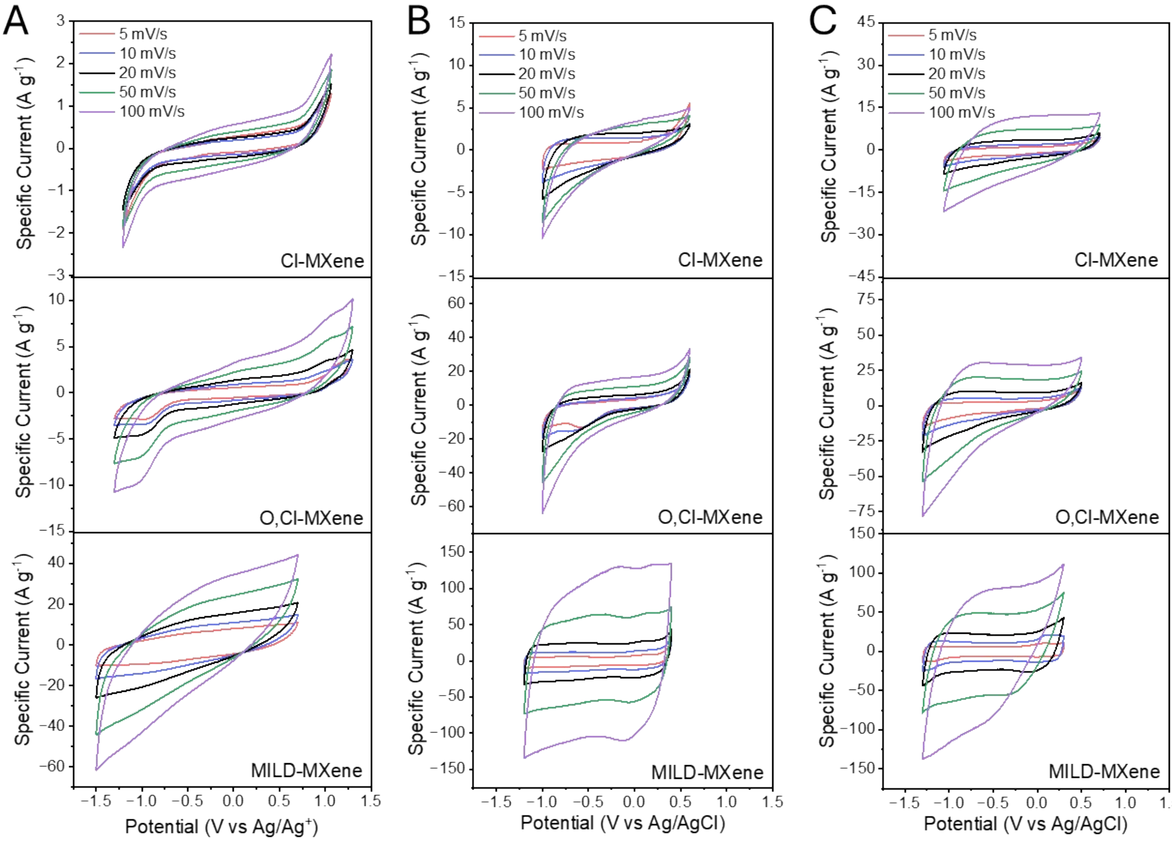

Fig. S5. Cyclic voltammograms of Cl-MXene, O,Cl-MXene, and MILD-MXene in (A) 1M LiTFSi in PC, (B) 1M aqueous LiCl, and (C) 1M aqueous KCl, done at their respective maximum stable operating voltage windows at 5, 10, 20, 50, and 100 mV s^{-1}.

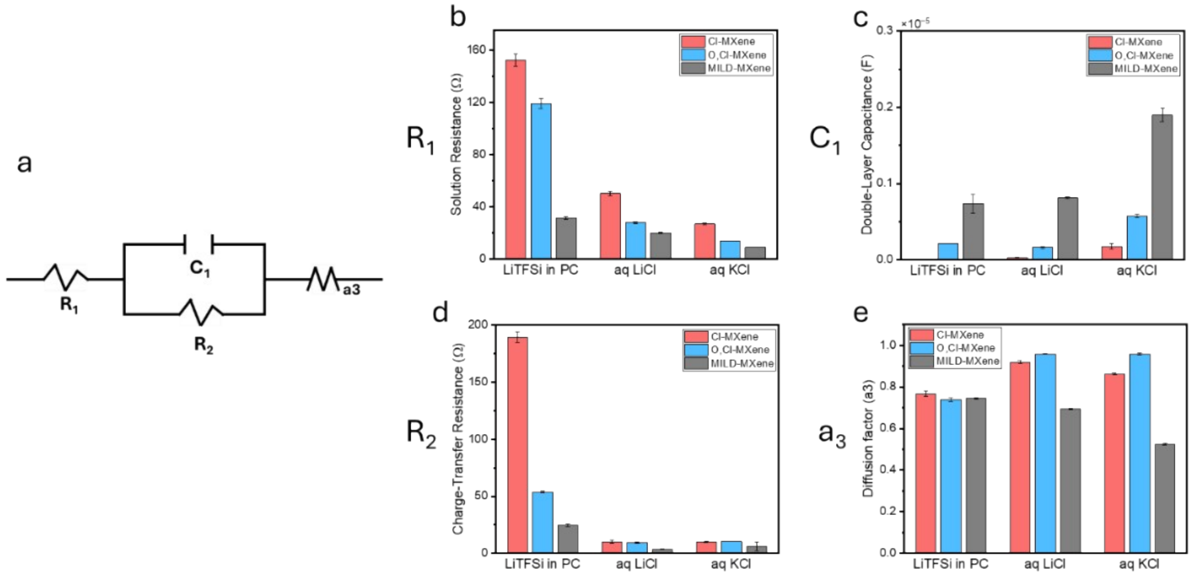

Fig. S6. (a) Randles-Ershler circuit model used for electrochemical impedance spectroscopic (EIS) analysis. (b) Equivalent series resistance, (c) double-layer capacitance, (d) charge-transfer resistance, and (e) diffusion factor obtained from the circuit model fitting.